Crystal structures of complexes of the small ribosomal subunit with tetracycline, edeine and IF3

Marta Pioletti[1,2], Frank Schlünzen[3], Jörg Harms[3], Raz Zarivach[4], Marco Glühmann[3], Horacio Avila[1,5], Anat Bashan[4], Heike Bartels[3], Tamar Auerbach[2,4], Carsten Jacobi[6], Thomas Hartsch[6], Ada Yonath[3,4] and François Franceschi[1,7]

[1]Max-Planck-Institut für Molekulare Genetik, Ihnestrasse 73, 14195 Berlin, [2]FB Biologie, Chemie, Pharmazie, Freie Universität Berlin, Takustrasse 3, 14195 Berlin, [3]Max-Planck-Research Unit for Ribosomal Structure, Notkestrasse 85, 22603 Hamburg, [6]Göttingen Genomics Laboratory, Georg-August Universität, Griesebacherstrasse 8, 37077 Göttingen, Germany, [4]Department of Structural Biology, Weizmann Institute, 76100 Rehovot, Israel and [5]Centro de Investigaciones Biomédicas, Universidad de Carabobo, Las Delicias, Maracay, Venezuela

[7]Corresponding author
e-mail: franceschi@molgen.mpg.de

M.Pioletti, F.Schlünzen and J.Harms contributed equally to this work

The small ribosomal subunit is responsible for the decoding of genetic information and plays a key role in the initiation of protein synthesis. We analyzed by X-ray crystallography the structures of three different complexes of the small ribosomal subunit of *Thermus thermophilus* with the A-site inhibitor tetracycline, the universal initiation inhibitor edeine and the C-terminal domain of the translation initiation factor IF3. The crystal structure analysis of the complex with tetracycline revealed the functionally important site responsible for the blockage of the A-site. Five additional tetracycline sites resolve most of the controversial biochemical data on the location of tetracycline. The interaction of edeine with the small subunit indicates its role in inhibiting initiation and shows its involvement with P-site tRNA. The location of the C-terminal domain of IF3, at the solvent side of the platform, sheds light on the formation of the initiation complex, and implies that the anti-association activity of IF3 is due to its influence on the conformational dynamics of the small ribosomal subunit.
Keywords: antibiotics/edeine/IF3/ribosomes/tetracycline

Introduction

The small ribosomal subunit (30S in prokaryotes) is responsible for decoding the genetic information. It plays a central role in the formation of the initiation complex, which requires its interaction with mRNA, initiator tRNA and the initiation factors. It also discriminates among aminoacyl tRNA molecules, thus ensuring translational fidelity. Hence, it is a natural target for ligands that inhibit protein biosynthesis, such as toxins and antibiotics.

Antibiotics are extremely versatile in their modes of action. They have three main bacterial targets: (i) bacterial cell-wall biosynthesis (β-lactamases, vancomycin); (ii) bacterial protein synthesis (macrolides, tetracyclines, aminoglycosides and oxazolidinones); and (iii) bacterial DNA replication and repair (fluoroquinolones) (Walsh, 2000). Universal antibiotics such as edeine or pactamycin inhibit protein synthesis in all phylogenetic kingdoms (Altamura *et al.*, 1988) and hence have little clinical relevance. However, deciphering their interactions with the ribosome helps in understanding the evolutionarily conserved aspects of protein synthesis. Structural information about ribosomal antibiotic-binding sites was first obtained by nuclear magnetic resonance (NMR) studies of complexes of antibiotic agents with fragments of 16S RNA (Fourmy *et al.*, 1996). Recently, the high resolution structures of the ribosomal subunits (Ban *et al.*, 2000; Schlünzen *et al.*, 2000; Wimberly *et al.*, 2000) have facilitated detailed elucidation of the actions of antibiotics *in situ* (Carter *et al.*, 2000; Nissen *et al.*, 2000).

Tetracycline is a product of the aromatic polyketide biosynthetic pathways and belongs to a family of bacteriostatic antibiotics that act against a wide variety of bacteria. Tetracyclines inhibit protein synthesis by interfering with the binding of aminoacylated tRNA (aa-tRNA) to the A-site of the 30S subunit (reviewed in Spahn and Prescott, 1996). However, ribosome-dependent GTP hydrolysis by elongation factor Tu (EF-Tu) is unaffected by tetracyclines. Hence, tetracyclines seem to have no effect on the initial binding of the ternary complex of EF-Tu and aa-tRNA to the A-site (Gordon, 1969).

The antibiotic edeine is a peptide-like compound produced by a strain of *Bacillus brevis*. Edeine contains a spermidine-type moiety at its C-terminal end and a β-tyrosine residue at its N-terminal end (Kurylo-Borowska, 1975). A subset of the 16S rRNA nucleotides protected by the P-site tRNA binding is also protected upon edeine binding (Moazed and Noller, 1987; Woodcock *et al.*, 1991). Edeine protects 16S rRNA at a site that overlaps with that of kasugamycin, which protects bases A794 and G926, and that of pactamycin, which protects bases G693 and C795 (Woodcock *et al.*, 1991; Mankin, 1997). Edeine acts on ribosomes of all kingdoms by affecting translation initiation (Odon *et al.*, 1978). The universal effect of edeine on initiation implies that structural elements important for the initiation process are universally conserved in prokaryotes and eukaryotes.

Initiation of translation is a complex process that requires, in prokaryotes, the binding of mRNA, three initiation factors (IF1, IF2-GTP and IF3), and initiator tRNA to the 30S subunit (Gualerzi and Pon, 1990). The formation of this initiation complex is strongly dependent on IF3, which influences the binding of the other ligands (Gualerzi and Pon, 1990). IF3 is a small basic protein of

Table I. Crystallographic statistics of data collection and refinement

Compound	Resolution (Å)	Number observed	Unique reflections	Completeness (%)	$<I>/<\sigma(I)>$	R_{sym} (%)	R/R_{free} (%)
Native	40–3.2	2 485 385	228 166	86.8 (83.2)	19.8 (2.0)	13.6 (38.1)	20.3/24.5
Tetracycline	35–4.5	365 437	79 036	89.7 (79.8)	9.1 (3.4)	9.9 (31.0)	22.3/25.4
Edeine	35–4.5	268 539	66 468	76.1 (68.2)	9.8 (2.5)	8.8 (41.8)	23.7/24.4
IF3C	35–4.2	417 631	83 090	81.5 (69.6)	9.2 (2.4)	9.9 (35.7)	20.5/26.4

Numbers in parentheses describe the highest resolution bin.

~20 kDa. It consists of a C-terminal domain (IF3C) and an N-terminal domain (IF3N) connected by a 20-residue-long, lysine-rich linker region. The structure of the whole protein has not been determined, but NMR and X-ray structures of the isolated linker region and N- and C-terminal domains have been reported (Biou *et al.*, 1995; Garcia *et al.*, 1995a,b). IF3C binds firmly to the small subunit, whereas its inter-domain linker and IF3N are loosely attached (Weiel and Hershey, 1981).

IF3 was identified as an anti-association factor because it binds with high affinity to the 30S subunit and thus prevents re-association of the 30S and 50S subunits (Grunberg-Manago *et al.*, 1975). IF3 shifts the dissociation equilibrium of the 70S ribosome towards free subunits, and favors the recycling of the 30S subunit. IF3C alone is able to prevent the association of the 30S with the 50S subunit (Hershey, 1987), whereas the ability of IF3 to discriminate non-canonical initiation codons, or to verify codon–anticodon complementarity, has been attributed mainly to IF3N (Bruhns and Gualerzi, 1980).

Here we report the structural analysis of three functionally relevant complexes of the 30S ribosomal subunit of *Thermus thermophilus* (T30S), with tetracycline, with edeine and with IF3C. We found six binding sites for tetracycline, one for edeine and one for IF3C. The locations of tetracycline and edeine allowed us to suggest how these antibiotics affect translation. The binding site of IF3C shows that its anti-association activity is connected to changes in the mobility of the 30S subunit and not to its binding at the inter-subunit interface.

Results

Structure determination

We determined and refined the 3.2 Å structure of the 30S subunit (Table I). This minor extension of the resolution of our previous 3.3 Å structure (Schlünzen *et al.*, 2000) led to a more complete model containing 1514 nucleotides and all 20 proteins (Figure 1). This model shows essentially the same RNA and protein folds (root mean square deviation 1 Å) as was determined independently by Wimberly *et al.* (2000), but several RNA bulges, hairpin loops and protein extensions have slightly different conformations. Detailed analysis of the refined structure will be published elsewhere.

This model was used to determine the structures of three functionally relevant complexes. These were obtained by soaking crystals of the 30S subunit of *T.thermophilus* in solutions containing tetracycline, edeine or IF3C. Here we describe the crystal structure of each of the three 30S complexes up to 4.2 Å resolution. The σA weighted

difference maps, calculated after refinement of the native structure against the observed structure factor amplitudes for each of the three complexes, confirmed the locations obtained from the difference Fourier between native and ligand data sets. Minor changes in the unit cell dimensions were observed for the soaked crystals (i.e. edeine: $a = b = 407.1$ Å, $c = 174.1$ Å; tetracycline: $a = b = 406.9$ Å, $c = 175.2$ Å; IF3C: $a = b = 407.5$ Å, $c = 174.8$ Å). The results of the refinement of the structures of the 30S complexes including the ligands are shown in Table I.

The resolution of the structures presented here limits our ability to deduce the exact chemical nature of the 30S–ligand interactions. In all cases, however, the electron density maps allowed unambiguous interpretations. Aided by the available biochemical and functional data, we propose mechanisms for selected events in the initiation process and for the modes of action of the antibiotics tetracycline and edeine.

Tetracycline

We identified six tetracycline-binding sites on the 30S subunit (Figure 1A), with relative occupancies ranging from 1 to 0.41 (Table II; Figure 2). Tet-1, the site with the highest occupancy, is located between the distorted minor groove of H34 and the stem–loop of H31, near to the A-site where the aa-tRNA (Cate *et al.*, 1999) was docked onto the 30S structure (Schlünzen *et al.*, 2000). The five additional tetracycline sites are found at various locations in the head and the upper half of the body (Table II; Figure 1A). The observation of multiple tetracycline-binding sites was not unexpected, since several binding sites for tetracycline had already been suggested by biochemical experiments (Table II).

The Tet-1-binding site is located in a pocket formed by residues 1054–1056 and 1196–1200 of H34, and 964–967 of H31 (Figure 2A). Bases 1196 and 1054, which are pointing out of H34 towards the A-site, form a clamp that holds the tetracycline molecule by hydrophobic interactions. Upon binding, the gap between these two bases becomes slightly wider. Aside from this local conformational change, we did not observe any significant changes of the 30S subunit. This finding is consistent with toeprinting experiments in the presence of tetracycline (Jerinic and Joseph, 2000). Tet-1 interacts with the sugar–phosphate backbone of H34. This interaction seems to be coordinated through a Mg^{2+} ion, in a fashion similar to the interaction between the Mg–tetracycline complex and the tetracycline repressor tet(R) (Orth *et al.*, 1999).

Tet-2 is located in a hydrophobic pocket of S4 (Figure 2B) and is the only tetracycline-binding site not
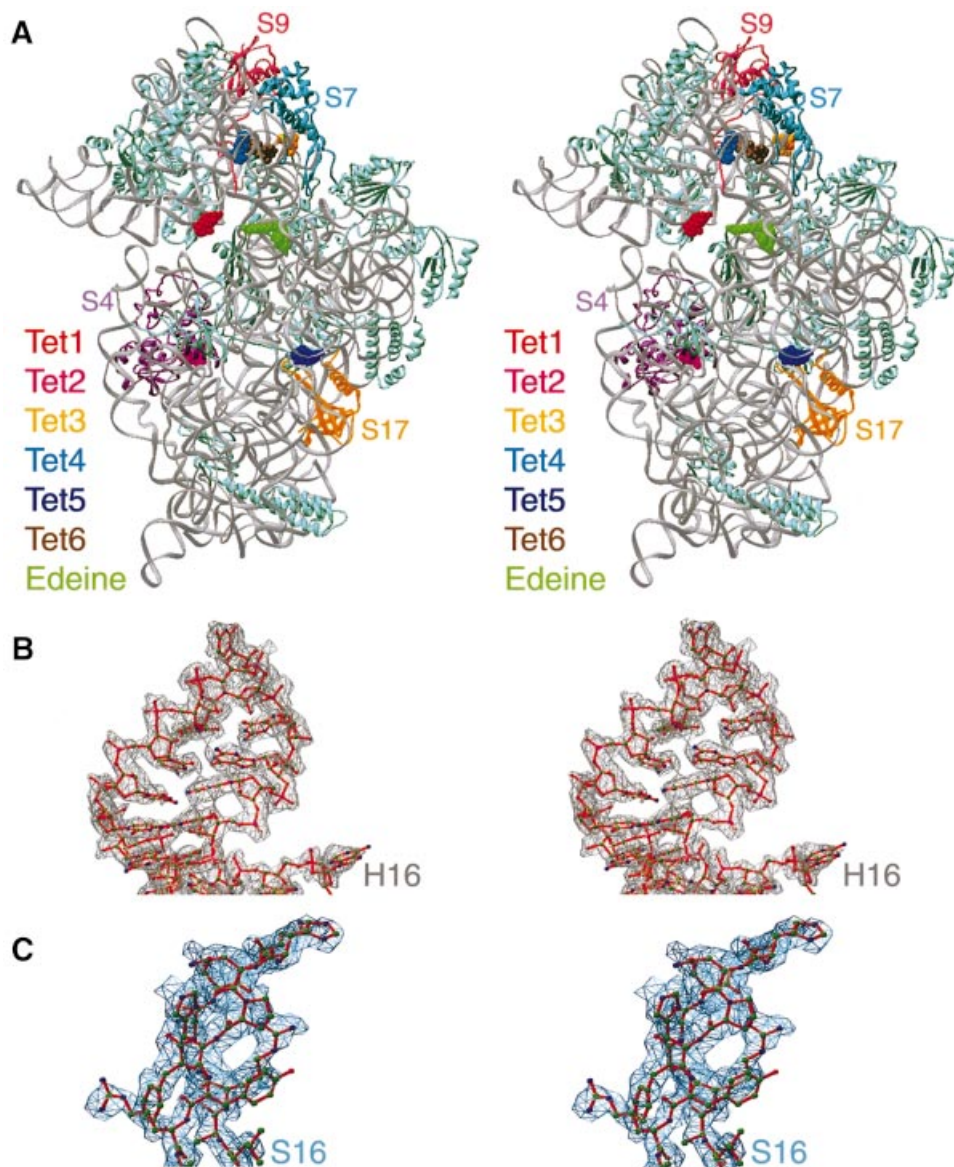
Fig. 1. (**A**) Stereo view of the 3.2 Å structure of the 30S ribosomal subunit. The binding sites of tetracycline and edeine are indicated. Ribosomal proteins interacting with tetracycline have been colored and labeled. (**B** and **C**) Stereo views of the electron density map of two regions of the 3.2 Å structure, corresponding to helix 16 (H16) and ribosomal protein S16, respectively.

involved in interactions with the 16S rRNA. This pocket is formed by a helix–loop–helix motif (residues 78–98 and 185–192). Arg187 and Lys85, which are not involved in RNA or protein–protein interaction, close the pocket on the hydrophilic side of tetracycline. Tet-3 is buried inside H40, between its stem–loop and its tetraloop (Figure 2C). The tetracycline interacts with U1159 of H40, which points back towards the tetraloop of H40, and the RNA residues adjacent to the tetraloop (1146/47 and 1153/54).

Tet-4 is located in a cavity formed by H29, H30 and H43 (Figure 2D). It interacts with the bases of RNA residues 941–943 of H29 and those of RNA residues 1342/43 of H43. Furthermore, it interacts with the RNA backbone of residues 1349/50 of H43 and G1233 of H30. Gln124 at the C-terminal end of S9 closes the cavity between H30 and H43. Tet-5 lies in a rather tight pocket confined by H11, H20, H27 and S17 (Figure 2E). The

hydrophilic side of tetracycline interacts with the phosphate–sugar backbone of residues 894/895 in the switch region of H27, and with the bulged bases U244, C245 and A246 of H11. Base G761 in H20 defines the other side of the pocket. Residues 99–101 in the C-terminal extension of S17, which is unique to thermophilic bacteria, are also involved in the binding. This site was revealed biochemically in mesophilic bacteria; therefore, it seems that the C-terminal tail of S17 is not essential for the binding of tetracycline at this site.

Tet-6 is located in the vicinity of the E-site, in a cavity defined by Arg4 and Arg5 at the N-terminal end of S7, Arg120 of S9, and helices H28, H34, H38 and H43 of 16S rRNA (Figure 2D). The interactions between rRNA and Tet-6 site are exclusively with the backbone of the RNA and are coordinated by a Mg^{2+} ion in a similar fashion to that observed for the Tet-1 site. These interactions involve

Table II. The crystallographically determined binding sites of tetracycline and edeine to the 30S ribosomal subunit, and the corresponding biochemical data

Ligand	Relative occupancy[a]	Location in the 30S structure	Biochemical data, <10Å distance
Tet-1	1.0	A964–G966 (H31), G1053, C1054 (H34), A1196–G1198 (H34)	enhanced reactivity of U1052 and U1054 (Moazed and Noller, 1987); tetracycline-resistant G1058C mutation (Ross *et al.*, 1998); inhibits cross-link of C967 × C1400 (Noah *et al.*, 1999)
Tet-2	0.7	Lys85, Val92–Leu96 and Leu188 (S4)	–
Tet-3	0.65	C1162–G1164 (H40), G1172–G1174 (H40)	–
Tet-4	0.53	G941,G942 (H29), C1342, G1343 (H29), A1349–U1351 (H43), Gln124 (S9)	cross-linked to G1338 (Oehler *et al.*, 1997)
Tet-5	0.41	U244–G247 (H11), G894–G896 (H27)	protection against chemical modification of A892 (Moazed and Noller, 1987); decreases the cross-link U244 × G894 (Noah *et al.*, 1999); cross-linked to G890 (Oehler *et al.*, 1997)
Tet-6	0.41	A937–A938 (H28/H29), C1378–U1380 (H28), Arg4, Arg5 (S7), Arg120 (S9)	photochemical cross-link: S7 (Goldman *et al.*, 1983); inhibits the cross-link of 967 × C1400 (Noah *et al.*, 1999)
Edeine	1.0	A790–A792(H24), G926 (H28), U1498, U1505 (H45) G693 × C795[b] (H23 × H24)	protection against chemical modification of G693, A794, C795, G926; weak protection of A790, G791, A1394 (Moazed and Noller, 1987)

[a]Relative occupancies are defined as fractions of the Tet-1 occupancy.
[b]Corresponds to the edeine-induced cross-helix base pair.

residues G933 and C934 of H28, G1186 in the single strand connecting H34 and H38, and U1345 and A1346 in the E-loop of H43. Overall, the binding of tetracycline to the Tet-6 site is dominated by the interaction of tetracycline with single-stranded 16S RNA regions and the apparently flexible extensions of S7 and S9. Thus, the stability of the tetracycline bound at Tet-6 and hence its occupancy could vary according to the experimental conditions, as indicated by biochemical data (Oehler *et al.*, 1997). Although Tet-6 is the site with the lowest relative occupancy, it can be correlated with many biochemical results (Table II).

Edeine

The complex of the 30S subunit with edeine revealed two strong peaks in the difference density maps, accounting for the binding site of edeine and the formation of a new RNA base pair. Edeine was located in the vicinity of the E-site, interacting with H24, H28, H44 and H45, and connecting universally conserved bases involved in the initiation process (Figures 1A and 2F). Docking the peptidyl-tRNA at the P-site of the 30S structure shows that the spermidine-like moiety of edeine interacts with the backbone of the tRNA. The interactions of edeine with the P-site tRNA could therefore explain the reduction of the affinity of the peptidyl-tRNA for the P-site.

The β-tyrosine part of edeine interacts with G926 in a way that mimics a regular RNA base pair. The position of edeine is further stabilized through its interactions with the backbone of the penultimate helix (H44), namely U1498, and G1505 in H45. RNA residues 790–792 in the loop of H24 interact mainly through their sugars with the hydrophobic side of edeine. These interactions result in a small distortion of H24, which is sufficient to induce a cross-helix base pairing between C795 in the loop of H24 and G693 in the loop of H23. The formation of this base pair might lead to an undesirable stabilization of the conformation of the platform, and in this way contribute to the inhibitory activity of edeine.

IF3

After refinement of the structure using the data of the 30S–IF3C complex, the difference Fourier map revealed density that allowed unambiguous accommodation of the two α-helices of IF3C, whereas the β-sheets and some side chains of IF3C are less well resolved. Neither the difference map nor the refinement of the complex indicated a significant conformational change in the 30S subunit upon IF3C binding.

In our map, IF3C lies at the upper end of the platform on the solvent side (Figure 3A and C). It is located between H23, H26 and the 3′ end of H45. In this location it would not physically block the interactions between the small and the large subunits. The contacts of IF3C with the 16S RNA involve the bulge of H23 (719–723), H26 (833–839) and the 3′ proximal end of H45 (1532–1534) close to the anti-Shine–Dalgarno (anti-SD) sequence. Additional contacts with the 30S subunit involve S2, S7, S11 and S18 (Figure 3C). Our results are consistent with those of cross-links of IF3 to 1506–1529 and 819–859 (Ehresmann *et al.*, 1986), and cross-links to proteins S7, S11 and S18 (Mackeen *et al.*, 1980).

Residues 21–31 in the flexible N-terminal end of S2 are in contact with the loop connecting B6 and α-H4 of IF3C (Figure 3C). S7 interacts with IF3C through its long C-terminal tail. This flexible part of S7 is partially organized in our structure by the heavy atom (W18) that was used by us for phasing (Tocilj *et al.*, 1999). Thus, it is possible that W18 interferes with the interactions between S7 and IF3C. Residues 87–96 of S11 interact mainly with B5 of IF3C (Figure 3C). The contact area between S18 and IF3C is rather large. Residues 7–18 of the N-terminal end of S18 wrap around IF3C and face its inner β-sheets; these S18 residues interact with IF3C residues 104–125 and 134–141 (*T.thermophilus* sequence). An additional contact is formed by residues 52–55 of S18 interacting with the loop between B5 and α-H3 of IF3C (Figure 3C). We found that the conformation of the N-terminal end of S18 depends on the soaking conditions of W18, indicating that this end of S18 is particularly flexible. Similarly, the
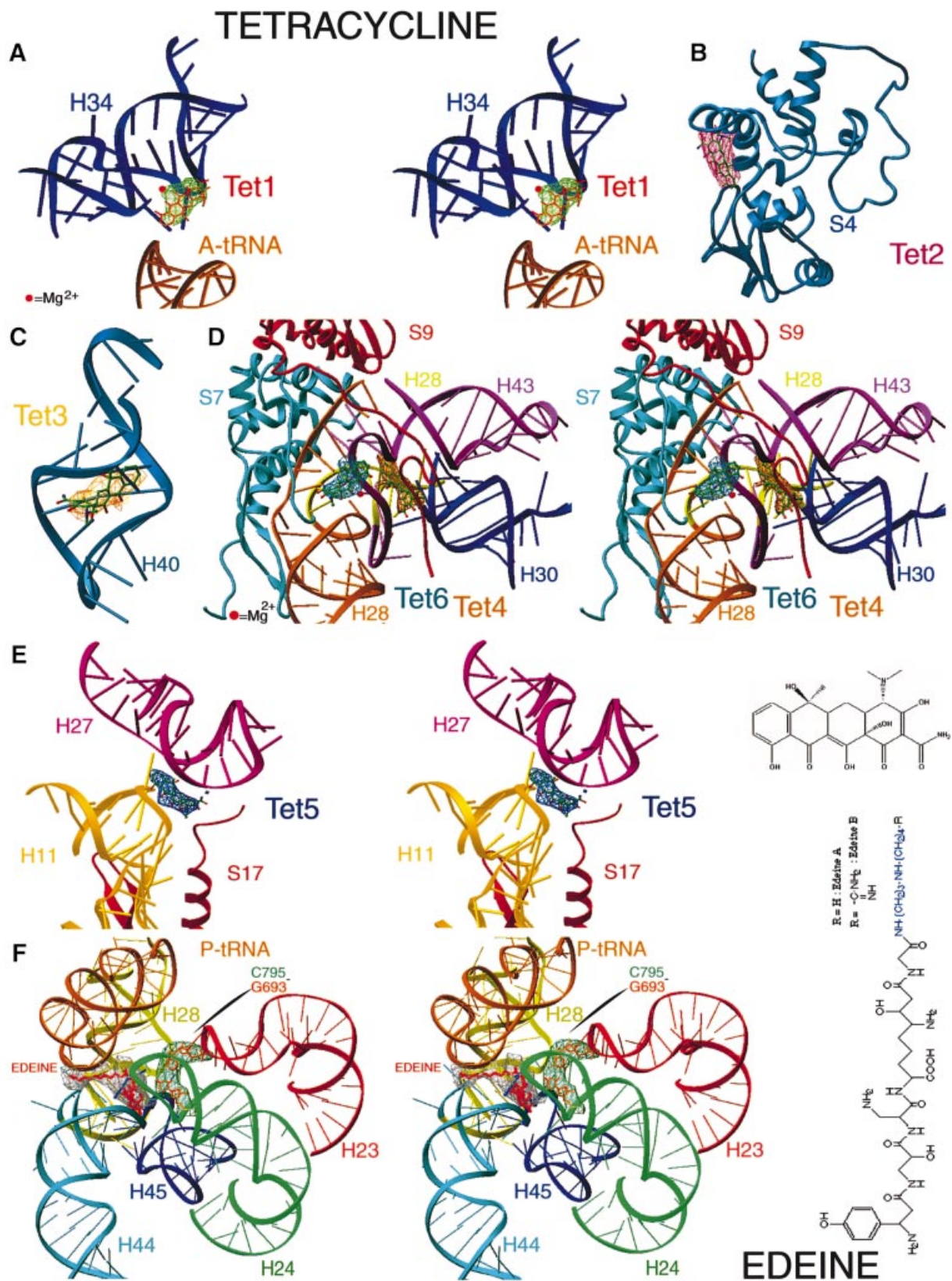
Fig. 2. Details of the binding sites of tetracycline and edeine. All images show the σA weighted difference density at contour levels ranging from 3.2 to 2.2σ for tetracycline, and 3.2σ for both edeine and the RNA base pair induced upon its binding. (**A**) Stereo view of Tet-1. (**B**) Mono view of Tet-2. (**C**) Mono view of Tet-3. (**D**) Stereo view of Tet-4 and -6. (**E**) Left: stereo view of Tet-5. Right: chemical structure of tetracycline. (**F**) Left: stereo view of the binding site of edeine. Right: chemical structure of edeine.
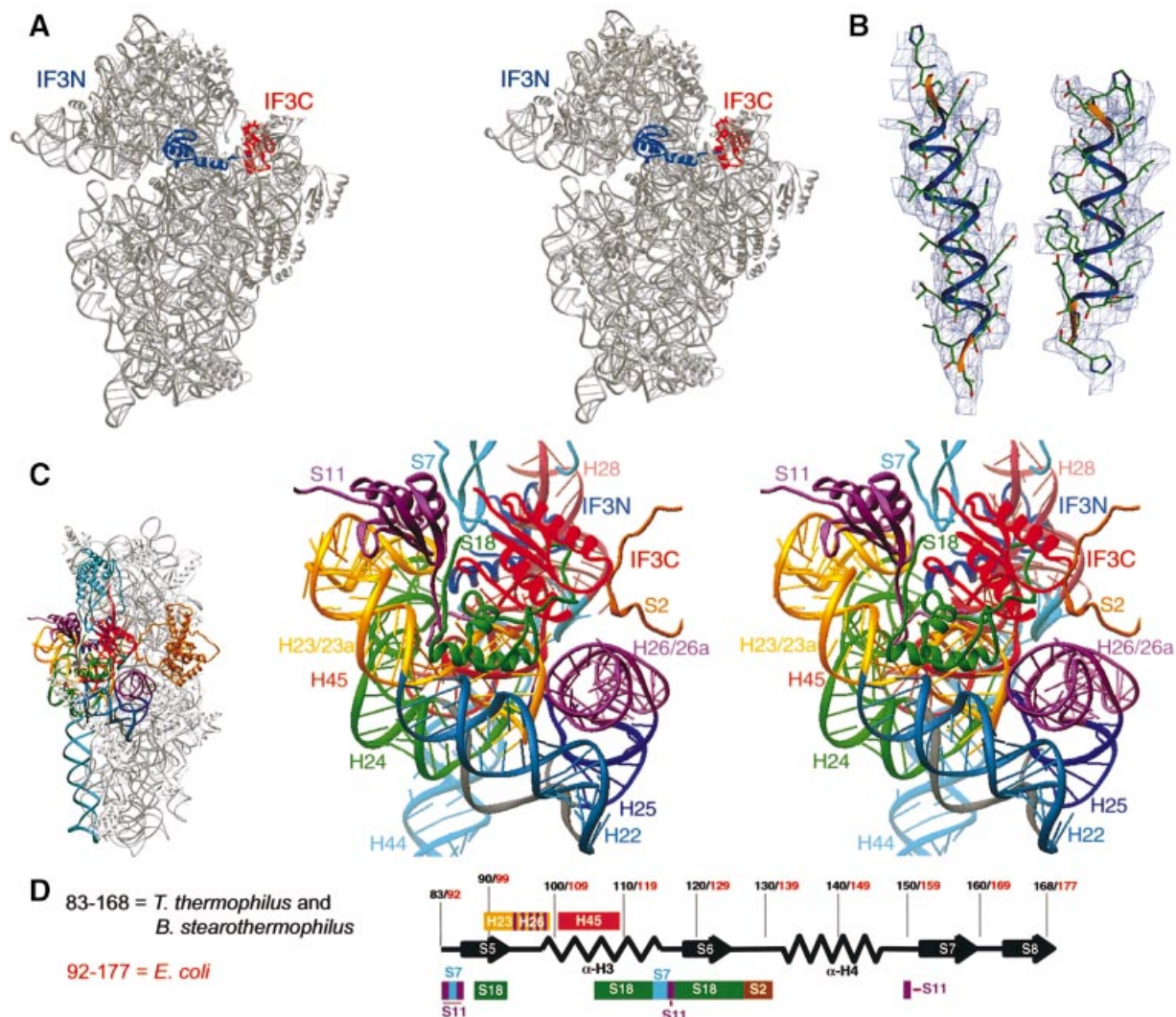
Fig. 3. Binding of IF3 to the small subunit. (**A**) The model of the complete 30S–IF3C complex (IF3C in red) and the docking of IF3N (blue) is shown. (**B**) Two regions of the σA weighted difference map contoured at 3σ. (**C**) Mono view of the 30S particle (on the left) having the same orientation as the stereo view of the model of the 30S–IF3 complex (on the right) in the vicinity of IF3C. Parts of the 30S structure not involved in the interactions with IF3 are omitted for clarity. (**D**) Secondary structure of IF3C. Residues of IF3C interacting with different RNA helices and ribosomal proteins are highlighted. Nomenclature of the secondary structure is based on Biou *et al.* (1995). Above the secondary structure diagram are the rRNA regions and below the diagram are the proteins that interact with IF3C.

N-terminal end of S2 and the C-terminal ends of S7 and S11 show different conformations in the two independently determined 30S structures (Schlünzen *et al.*, 2000; Wimberly *et al.*, 2000), indicating that these protein extensions are rather flexible. Thus, these protein extensions appear to act as tentacles, which enhance the binding and placement of ribosomal factors like IF3.

NMR and mutagenesis studies of IF3 showed that in *Escherichia coli* residues 99–116, 127–137, 145–155 and 168 are involved in IF3 binding to the 30S subunit (Sette *et al.*, 1999). It was suggested that residues 99, 112 and 116 are the major RNA-binding residues, whereas 131–137 are the residues involved in IF3C–protein contacts (Sette *et al.*, 1999). The results of these studies are consistent with the interactions that we observed by analyzing the structure of the 30S–IF3C complex (Figure 3C).

We attempted the docking of IF3N to the 30S subunit so that its proposed function, the constraints imposed by the

position of IF3C and the existing biochemical data were all satisfied. Docking was performed manually as well as with MOLFIT (Eisenstein *et al.*, 1997) and the only location on the 30S subunit that could fulfill all these requirements was found in close proximity to the P-site (Figure 3A). In this position, IF3N interacts with H28, H29, H31, H34 and H44 (via nucleotides 924–927 and 1381–1387 of H28, 1341 of H29, 966–968 of H31, 1062–1064 of H34 and 1398–1400 of H44). IF3N hence contacts all helices known to be involved in the peptidyl-tRNA binding and could affect the RNA cross-links C967 × C1400 and C1402 × C1501, as reported (Shapkina *et al.*, 2000).

The binding of IF3N leaves only a limited space for P-site tRNA, and requires small conformational changes for simultaneous binding of both IF3N and P-site tRNA. This could shed light on the mechanism of IF3N-mediated discrimination of non-canonical initiation codons or codon–anticodon complementarity. Docking the P-site tRNA into this model (Cate *et al.*, 1999) shows close

contacts between tRNA residues 31–35 and the N-terminal end of IF3N, which could also explain the effect of IF3N on the P-site tRNA cross-links (Shapkina *et al*., 2000).

Discussion

Tetracycline

We have identified six binding sites for tetracycline in the 30S subunit (Table II; Figure 1A) but found no common structural trait among the binding sites. The questions arise, which sites could affect translation and to what extent are they involved in the inhibitory action of tetracycline? Tet-1, the site with the highest relative occupancy (Table II; Figure 2A), interferes with the location where the A-site tRNA (Cate *et al*., 1999) was docked onto the 30S structure (Schlünzen *et al*., 2000). Thus, tetracycline can physically prevent the binding of the tRNA to the A-site. This mode of interaction is consistent with the classical model of tetracycline as an inhibitor of A-site occupation, and hence offers a clear explanation for the bacteriostatic effect of tetracycline.

There are two ribosome-related mechanisms of tetracycline resistance in bacteria. Both are linked to the Tet-1 site. In one, resistance is mediated by ribosomal protection proteins (Roberts, 1996) and in the other by the mutation 1058G→C on 16S rRNA (Ross *et al*., 1998). Ribosomal protection proteins, such as TetM, TetO and TetS, confer resistance only at low concentrations of tetracycline, and show some sequence and structural homology with the elongation factors G and EF-Tu (Dantley *et al*., 1998). It has been proposed that TetM binds to the A-site and upon GTP hydrolysis actively releases the tetracycline bound to it (Dantley *et al*., 1998). The G1058→C mutation could hamper the base pairing of G1058 with U1199 and might lead to a conformational change that results in closing the Tet-1-binding pocket. This conformational change may be due to the release of the coordinating Mg^{2+} ion.

These two tetracycline resistance mechanisms reflect the importance of the Tet-1-binding site in the antibiotic action of tetracycline. However, the presence of five additional binding sites, the biochemical evidence for different locations of tetracycline and the low level of resistance conferred by the ribosomal protection proteins demand more complex explanations about the possible functional relevance of the five additional sites. Binding of tetracycline to Tet-4, -5 and -6 sites is supported by biochemical evidence (Table II), but there are no biochemical data on Tet-2 and -3 sites. The Tet-5 site is located between H11 and H27, the switch helix (Lodmell and Dahlberg, 1997), which is a functional hot spot (Figure 2E). Tetracycline bound to the Tet-5 position could limit the mobility needed by H27 to switch between the 912–885, or error prone conformation, and the 912–888, or restrictive conformation (Lodmell and Dahlberg, 1997). Therefore, tetracycline bound at Tet-5 could lock the 30S subunit into one of these two conformations.

Only four proteins, namely S4 for Tet-2, S7 for Tet-6, S9 for Tet-4 and -6, and S17 for Tet-5, come into contact with tetracycline. S4, S7, S9 and S17 are primary rRNA-binding proteins (Held *et al*., 1974). S4 and S7 are the two proteins that initiate the assembly of the 30S subunit (Nowotny and Nierhaus, 1988). Therefore, tetracycline

binding at the Tet-2, -4, -5 and -6 sites may not influence the decoding process, but could disturb the early assembly steps of new 30S particles, contributing to the overall inhibitory effect of tetracycline.

Overall, our data for the six positions can explain well the sometimes contradictory reported biochemical and functional data for tetracycline binding to the 30S subunits (Table II). We show that physical blockage of the A-site tRNA binding by tetracycline bound at Tet-1 can account for the inhibitory action of tetracycline, but we can not say with certainty that any of the five minor sites is involved in tetracycline action. Nevertheless, we hypothesize that, with the exception of tetracycline at the Tet-3 site, these sites could act synergistically to contribute to the bacteriostatic effect of tetracycline.

Edeine

We found one 30S-binding site for edeine (Figures 1A and 2F), in contrast to the six sites of tetracycline. All the rRNA bases defining the edeine-binding site are conserved in chloroplasts, mitochondria and the three phylogenetic domains, explaining why edeine is said to be a universal protein synthesis inhibitor (Altamura *et al*., 1988). Interestingly, the 16S rRNA bases involved in edeine binding are also conserved in *B.brevis*, the organism that synthesizes it. Thus, edeine acts equally well as a protein synthesis inhibitor on *B.brevis* ribosomes (Kurylo-Borowska, 1975), which resolves this apparent paradox by rapidly releasing the active edeine into the growth medium, and by only maintaining low concentrations of inactive edeine attached to the internal part of the cell membrane (Kurylo-Borowska, 1975).

The binding of edeine involves nucleotides situated in H24, H28, the neck helix, H44, the core of the decoding region and in its close neighbor H45, which is also involved in the decoding process (Figure 2F). Mutations in G791 and A792 (H24) reduce association of the 30S and 50S subunits, and an A792 mutant is associated with loss of IF3 binding (Tapprich *et al*., 1989; Santer *et al*., 1990). G926 (H28) interacts with the tRNA bound at the P-site and is protected by edeine (Woodcock *et al*., 1991). Furthermore, mutations in U1498 impair A-site function and enhance tRNAfMet selectivity (Ringquist *et al*., 1993), while mutations in G1505 increase the levels of stop codon read-through and frameshifting (O'Connor *et al*., 1995, 1997). By physically linking these four helices, critical points for tRNA, IF3 and mRNA binding, edeine could lock the small subunit in a fixed configuration and hinder the conformational changes that are thought to accompany the translation process (Gabashvili *et al*., 1999b; VanLoock *et al*., 2000).

In addition to the direct interactions of edeine with the 16S bases (Table II), our structure shows that edeine induces the formation of a base pair between C795 at the loop of H24 and G693 at the loop of H23 (Figure 2F). Although neither G693 nor C795 is directly involved in edeine binding, G693 has been shown to be protected when edeine is bound (Woodcock *et al*., 1991). Thus, the formation of this base pair explains the protection against chemical attack of G693 upon edeine binding.

H23 plays an important role in the binding of the C-terminal domain of IF3 (Table II), and nucleotides 787–795 of H24 are directly involved in 30S–50S subunit

association (Tapprich and Hill, 1986). Analysis of our structure shows that the G693–C795 base pair would impose constraints on the mobility of the platform, which is believed to move during translation (Gabashvili *et al.*, 1999a). Based on these findings, it is conceivable that the formation of the G693–C795 base pair interferes substantially with both elongation and initiation. Existing biochemical data on edeine binding to the 30S subunit support this hypothesis. These data suggest that edeine blocks not only initiation (Odon *et al.*, 1978), but also elongation, by interfering with the P-site tRNA (Moazed and Noller, 1987). It is possible that in prokaryotes and Archaea, the G693–C795 base pair blocks the path of the mRNA between the decoding region and the anti-SD region of the 16S rRNA.

This blockage would make the anti-SD region on the 16S rRNA less accessible and thus it would not base pair with the incoming mRNA during the initial stages of initiation. This effect on the mRNA path seems to be universal since edeine interacts with G926 and G693, two universally conserved nucleotides. G926 (H28) has been photo-cross-linked in *E.coli* to position +2 of the mRNA (Sergiev *et al.*, 1997) and to position +1 in human ribosomes (Demeshkina *et al.*, 2000). G693, on the other hand, has been photo-cross-linked in *E.coli* to positions –1/–3 of the mRNA (Bhangu and Wollenzien, 1992) and in human ribosomes to position –3 of the mRNA (Demeshkina *et al.*, 2000).

The only mutant resistant to edeine that has been functionally characterized is a mutant of *Saccharomyces cerevisiae*. This mutant overcomes edeine inhibition by an increased affinity for mRNA (Herrera *et al.*, 1984). In eukaryotes, where the initial docking of the mRNA is independent of base complementarity between the mRNA and the 18S rRNA, an increased affinity of the small subunit for mRNA could indeed promote edeine resistance. The cross-link of G693 with positions –1/–3 of the mRNA, together with the formation of the cross-helix base pair (G693–C795) induced by edeine in our structure, offer a good explanation as to why edeine interferes with the AUG recognition process in eukaryotes. It was shown that in the presence of edeine the 40S ribosome complex (tRNA–eIF2–GTP and other factors) scans along the mRNA without recognizing the AUG start codon (Kozak and Shatkin, 1978). The structure of the 30S–edeine complex shows that the path of the mRNA is altered, mainly in the region of the small subunit that should interact with the mRNA initiation codon, and thus should hamper the formation of the 80S initiation complex. Based on these findings, we conclude that the effect of edeine is to alter the path of the mRNA through the small ribosomal subunit, thereby affecting initiation as well as tRNA binding to the P-site and possibly even to the E-site.

In summary, our structural results are not only consistent with the biochemical data on edeine binding, but can also explain the involvement of edeine in the inhibition of the initiation and elongation processes. Our data suggest that the initiation process is the main target of this universal antibiotic. The fact that edeine induces an allosteric change of this nature—forming a new base pair—could be an important principle of antibiotic action never reported previously.

IF3

IF3C binds to the 30S particle at the upper end of the platform on the solvent side of 30S (Figure 3A), close to the anti-SD region of the 16S rRNA. IF3C does not bind at the inter-subunit interface of the 30S and 50S subunits, and therefore its anti-association activity is not the product of physical blockage at the interface between the two subunits.

EM reconstructions of rat liver 40S in complex with the eukaryotic initiation factor 3 (eIF3) located eIF3 in a comparable region at the upper edge of the platform (Srivastava *et al.*, 1992). The agreement with our results indicates that certain mechanisms underlying the initiation process have been evolutionarily conserved. This hypothesis is also supported by the results obtained for the 30S–edeine complex. In contrast, a more recent cryo-EM study on the *Thermus* small ribosomal subunit (McCutcheon *et al.*, 1999) localized IF3C on the side of the platform facing the subunit interface, suggesting a different mechanism for IF3C action.

Based on the location of IF3C that we observed, it is likely that the binding of IF3C to the 30S subunit influences the mobility of H45. The binding at this site could affect the conformational dynamics and thus prevent the association of the two ribosomal subunits. Our suggestion is supported by the observation that the double mutant of G1530/A1531 to A1530/G1531 in H45 of the 16S rRNA reduces IF3 binding to the 30S subunit 10-fold (Firpo *et al.*, 1996). Moreover, this double mutant enhances IF3 affinity for the 70S ribosomes, and IF3 is unable to promote the dissociation of 70S ribosomes carrying this mutation (Firpo *et al.*, 1996). Our structural results are consistent with these biochemical observations and support the hypothesis that IF3C binding alone is not sufficient to prevent subunit association or promote dissociation, but rather it acts by changing the conformational dynamics of the subunit. These results also support our finding that IF3C does not physically block the inter-subunit interface between the 30S and 50S subunit.

The spatial proximity of the IF3C-binding site to the anti-SD region of the 16S rRNA suggests a connection between IF3C binding and mRNAs interacting with the anti-SD region. The interaction of mRNA with the anti-SD region and with IF3 could suppress the change in the conformational dynamics induced by IF3, thus allowing subunit association. This could also explain the observation that leaderless mRNAs are only translated at low intracellular concentrations of IF3 (Tedin *et al.*, 1999). In the absence of the leader sequence (SD), the change in conformational dynamics induced by IF3 would not be reversed, and thus subunits will not be able to form the 70S initiation complex.

It has been suggested that the flexibility and the ability of the linker region to alter its fold are partially related to the function of IF3 in the formation of the initiation complex, and thus it has a functional importance. Assuming that our IF3N placement is correct, the linker region between IF3C and IF3N needs to be flexible. Indeed, the extreme flexibility of the linker region of IF3 was shown biochemically (de Cock *et al.*, 1999) as well as by NMR studies (Moreau *et al.*, 1997). Our results also agree with the proposal that the linker maintains its flexibility when IF3 is bound to the 30S subunit. Thus, it is

possible that once the IF3N and IF3C domains are bound, the linker acts as a strap between the two domains. In this manner, the IF3 linker could indirectly affect the conformation of the P-site and induce its specificity for tRNAfMet (de Cock *et al*., 1999). The location of the docked IF3N (Figure 3A) suggests that codon–anticodon recognition may be based on space-exclusion principles, rather than specific interactions of IF3 with the codon–anticodon complementarity mechanism, as suggested (Meinnel *et al*., 1999).

In summary, our localization of IF3C on the 30S subunit and the modeling of the linker region and of the IF3N-binding site provide a connection between IF3 function and the existing biochemical data. Our IF3C location (Figure 3C) shows clearly that the anti-association activity of IF3 is not due to physical blockage of the inter-subunit interface, but rather to a change in the conformational dynamics of the subunit. It also explains the correlation between the binding of IF3 to the small ribosomal subunit and the mRNA requirement to interact with the anti-SD region of 16S rRNA for efficient translation.

A related crystallographic study (Brodersen *et al*., 2000) was published during the reviewing period of this manuscript. It reports the binding of three antibiotics: tetracycline, for which two sites were revealed; pactamycin, which shares a similar chemical protection pattern to edeine; and hygromycin. Initial inspection shows considerable similarities between the reported tetracycline-binding sites and Tet-1 and -5 resolved by us. It also shows that pactamycin binding bridges H23 and H24 while edeine induces a base pair having the same bridging effect. The agreement between these independently obtained results confirms the reliability of both studies and shows clearly that the high resolution structure of the small ribosomal subunit offers excellent possibilities for illuminating the molecular bases for the modes of action of antibiotics and various other factors that affect ribosomal function.

Materials and methods

Orientation
Unless stated otherwise, throughout this article the long axis of the 30S subunit is oriented vertically. In all figures, the head is at the top of the drawing, with the 50S binding site facing the reader, so that the shoulder of the 30S subunit is on the left and the platform on the right hand side. This orientation is also used to describe the ligand orientation with respect to the 30S subunit.

Base numbering
Bases are numbered according to the *E.coli* 16S rRNA sequence, unless stated otherwise. Helices are numbered as described by Mueller and Brimacombe (1997).

Preparation of T.thermophilus IF3C
The region of the *infC* gene coding for amino acids 71–171 of IF3 was amplified using PCR. The PCR products were inserted into the expression vector pET11a. This construct was then transformed into *E.coli* BL21(DE3)pLysS. IF3C overproduction was induced with 1 mM isopropyl-β-D-thiogalactopyranoside. The cell lysate was heated at 60°C for 30 min, and denatured proteins were removed by centrifugation. The supernatant containing IF3C was passed over a DEAE–Sepharose column. IF3C fractions were further purified to 98% purity by Resource S and a Phenyl-Superose column.

T30S crystals
Crystals of T30S belonging to the tetragonal space group $P4_12_12$ ($a = b = 406.3$ Å; $c = 173.1$ Å) were grown and treated as described

(Tocilj *et al*., 1999). Soaking was performed in two steps, initially at 40°C and then at 23°C, in solutions containing 20 μM IF3C, 4 μM tetracycline (4-[dimethylamino]-1,4,4a,5,5a,6,11,12a-octahyrdo-3,6,10,12,12a-penta-hydroxy-6-methyl-1,11) or 5 μM edeine (β-tyrosyl-*N*-isoseryl-N^2-diaminopropanyl-N^2-2,6-diamino-7-hydroxyazelyl-glycyl-spermidine).

X-ray diffraction
Data were collected at 85 K from shock-frozen crystals with bright SR beam at ID19 at APS/SBC, ID14/2&4 at ESRF/EMBL, and at BW6&7 at DESY. Data were recorded on MAR345, Quantum 4 or APS-CCD detectors and processed with HKL2000 (Otwinowski and Minor, 1997).

T30S sequences
Unpublished sequences of T30S proteins and of *T.thermophilus* IF3 were provided by C.Jacobi and T.Hartsch of the Göttingen Genomics Laboratory, Göttingen, Germany.

Placements and refinement
The 3.2 Å native structure of the 30S subunit was refined against the structure factor amplitudes of each of the three ligand–30S complexes, using rigid body refinement as implemented in CNS (Brünger *et al*., 1998). Unweighted, as well as σA weighted, difference maps were used for the initial manual placement of the ligands. Each of the three ligand–30S models was further refined in CNS. For the calculation of free *R*-factor (as reported in Table I) the same subset of reflections (10% of the data) was omitted from the refinement. The coordinates of the refined structure and of the three complexes were submitted to the Protein Data Bank (PDB) (accession codes 1I94, 1I95, 1I96 and 1I97).

Coordinates
Coordinates of IF3 were taken from the PDB (1TIG and 1TIF). Tetracycline was modeled into the difference density based on its crystal structure (PDB code 2TRT). Edeine was modeled into the difference density by combining chemical structure information (Kurylo-Borowska, 1975) with three-dimensional geometry.

Figures
All figures were produced with RIBBONS (Carson, 1997).

References

Altamura,S., Sanz,J.L., Amils,R., Cammarano,P. and Londei,P. (1988) The antibiotic sensitivity spectra of ribosomes from the Thermoproteales: phylogenetic depth and distribution of antibiotic binding sites. *Syst. Appl. Microbiol.*, **10**, 218–225.

Ban,N., Nissen,P., Hansen,J., Moore,P. and Steitz,T. (2000) The complete atomic structure of the large ribosomal subunit at 2.4 Å resolution. *Science*, **289**, 905–920.

Bhangu,R. and Wollenzien,P. (1992) The mRNA binding track in the *Escherichia coli* ribosome for mRNAs of different sequences. *Biochemistry*, **31**, 5937–5944.

Biou,V., Shu,F. and Ramakrishnan,V. (1995) X-ray crystallography shows that translational initiation factor IF3 consists of two compact α/β domains linked by an α-helix. *EMBO J.*, **14**, 4056–4064.

Brodersen,D.E., Clemons,W.M., Carter,A.P., Morgan-Warren,R.J., Wimberly,B.T. and Ramakrishnan,V.R. (2000) The structural basis

for the action of the antibiotics tetracycline, pactamycin and hygromycin B on the 30S ribosomal subunit. *Cell*, **103**, 1143–1154.

Bruhns,J. and Gualerzi,C. (1980) Structure–function relationship in *Escherichia coli* initiation factors: role of tyrosine residues in ribosomal binding and functional activity of IF-3. *Biochemistry*, **19**, 1670–1676.

Brünger,A.T. *et al.* (1998) Crystallography & NMR system: A new software suite for macromolecular structure determination. *Acta Crystallogr. D*, **54**, 905–921.

Carson,M. (1997) Ribbons. *Acta Crystallogr. B*, **277**, 493–505.

Carter,A., Clemons,W., Brodersen,D., Morgan-Warren,R., Wimberly,B. and Ramakrishnan,V. (2000) Functional insights from the structure of the 30S ribosomal subunit and its interactions with antibiotics. *Nature*, **407**, 340–348.

Cate,J.H., Yusupov,M.M., Yusupova,G.Z., Earnest,T.N. and Noller,H.F. (1999) X-ray crystal structures of 70S ribosome functional complexes. *Science*, **285**, 2095–2104.

Dantley,K.A., Dannelly,H.K. and Burdett,V. (1998) Binding interaction between Tet(M) and the ribosome: requirements for binding. *J. Bacteriol.*, **180**, 4089–4092.

de Cock,E., Springer,M. and Dardel,F. (1999) The interdomain linker of *Escherichia coli* initiation factor IF3: a possible trigger of translation initiation specificity. *Mol. Microbiol.*, **32**, 193–202.

Demeshkina,N., Repkova,M., Ven'yaminova,A., Graifer,D. and Karpova,G. (2000) Nucleotides of 18S rRNA surrounding mRNA codons at the human ribosomal A, P and E sites: A crosslinking study with mRNA analogs carrying an aryl azide group at either the uracil or the guanine residue. *RNA*, **6**, 1727–1736.

Ehresmann,C., Moine,H., Mougel,M., Dondon,J., Grunbergmanago,M., Ebel,J.P. and Ehresmann,B. (1986) Cross-linking of initiation factor IF3 to *Escherichia coli* 30S ribosomal subunit by *trans*-diamminedichloroplatinum(II): characterization of two cross-linking sites in 16S rRNA; a possible way of functioning for IF3. *Nucleic Acids Res.*, **14**, 4803–4821.

Eisenstein,M., Shariv,I., Koren,G., Friesem,A.A. and Katchalski-Katzir,E. (1997) Modeling supra-molecular helices: extension of the molecular surface recognition algorithm and application to the protein coat of the tobacco mosaic virus. *J. Mol. Biol.*, **266**, 135–143.

Firpo,M.A., Connelly,M.B., Goss,D.J. and Dahlberg,A.E. (1996) Mutations at two invariant nucleotides in the 3′-minor domain of *Escherichia coli* 16S rRNA affecting translational initiation and initiation factor 3 function. *J. Biol. Chem.*, **271**, 4693–4698.

Fourmy,D., Recht,M.I., Blanchard,S.C. and Puglisi,J.D. (1996) Structure of the A site of *Escherichia coli* 16S ribosomal RNA complexed with an aminoglycoside antibiotic. *Science*, **274**, 1367–1371.

Gabashvili,I.S., Agrawal,R.K., Grassucci,R. and Frank,J. (1999a) Structure and structural variations of the *Escherichia coli* 30 S ribosomal subunit as revealed by three-dimensional cryo-electron microscopy. *J. Mol. Biol.*, **286**, 1285–1291.

Gabashvili,I.S., Agrawal,R.K., Grassucci,R., Squires,C.L., Dahlberg, A.E. and Frank,J. (1999b) Major rearrangements in the 70S ribosomal 3D structure caused by a conformational switch in 16S ribosomal RNA. *EMBO J.*, **18**, 6501–6507.

Garcia,C., Fortier,P., Blanquet,S., Lallemand,J.Y. and Dardel,F. (1995a) ¹H and ¹⁵N resonance assignment and structure of the N-terminal domain of *Escherichia coli* initiation factor 3. *Eur. J. Biochem.*, **228**, 395–402.

Garcia,C., Fortier,P., Blanquet,S., Lallemand,J.-Y. and Dardel,F. (1995b) Solution structure of the ribosome-binding domain of *E.coli* translation initiation factor IF3. Homology with the U1A protein of the eukaryotic spliceosome. *J. Mol. Biol.*, **254**, 247–259.

Goldman,R.A., Hasan,T., Hall,C.C., Strycharz,W.A. and Cooperman, B.S. (1983) Photoincorporation of tetracycline into *Escherichia coli* ribosomes. Identification of the major proteins photolabeled by native tetracycline and tetracycline photoproducts and implications for the inhibitory action of tetracycline on protein synthesis. *Biochemistry*, **22**, 359–368.

Gordon,J. (1969) Hydrolysis of guanosine 5′-triphosphate associated with binding of aminoacyl transfer ribonucleic acid to ribosomes. *J. Biol. Chem.*, **244**, 5680–5686.

Grunberg-Manago,M., Dessen,P., Pantaloni,D., Godefroy-Colburn,T., Wolfe,A.D. and Dondon,J. (1975) Light-scattering studies showing the effect of initiation factors on the reversible dissociation of *Escherichia coli* ribosomes. *J. Mol. Biol.*, **94**, 461–478.

Gualerzi,C.O. and Pon,C.L. (1990) Initiation of mRNA translation in prokaryotes. *Biochemistry*, **29**, 5881–5889.

Held,W.A., Ballou,B., Mizushim,S. and Nomura,M. (1974) Assembly

mapping of 30S ribosomal proteins from *Escherichia coli*. Further studies. *J. Biol. Chem.*, **249**, 3103–3111.

Herrera,F., Moreno,N. and Martinez,J.A. (1984) Increased ribosomal affinity for mRNA causes resistance to edeine in a mutant of *Saccharomyces cerevisiae. Eur. J. Biochem.*, **145**, 339–344.

Hershey,J.W. (1987) Protein synthesis. In Neidhardt,F., Ingraham,J., Low,K., Magasanik,B., Schaechter,M. and Umbarger,H. (eds), *Escherichia coli and Salmonella typhimurium: Cellular and Molecular Biology*. ASM, Washington, DC, pp. 613–647.

Jerinic,O. and Joseph,S. (2000) Conformational changes in the ribosome induced by translational miscoding agents. *J. Mol. Biol.*, **304**, 707–713.

Kozak,M. and Shatkin,A.J. (1978) Migration of 40S ribosomal subunits on messenger RNA in the presence of edeine. *J. Biol. Chem.*, **253**, 6568–6577.

Kurylo-Borowska,Z. (1975) Biosynthesis of edeine. II. Localization of edeine synthetase within *Bacillus brevis* Vm4. *Biochim. Biophys. Acta*, **399**, 31–41.

Lodmell,J.S. and Dahlberg,A.E. (1997) A conformational switch in *Escherichia coli* 16S ribosomal RNA during decoding of messenger RNA. *Science*, **277**, 1262–1267.

Mackeen,L.A., Kahan,L., Wahba,A.J. and Schwartz,I. (1980) Photochemical cross-linking of initiation factor-3 to *Escherichia coli* 30S ribosomal subunits. *J. Biol. Chem.*, **255**, 526–531.

Mankin,A.S. (1997) Pactamycin resistance mutations in functional sites of 16S rRNA. *J. Mol. Biol.*, **274**, 8–15.

McCutcheon,J.P., Agrawal,R.K., Philips,S.M., Grassucci,R.A., Gerchman,S.E., Clemons,W.M., Ramakrishnan,V. and Frank,J. (1999) Location of translational initiation factor IF3 on the small ribosomal subunit. *Proc. Natl Acad. Sci. USA*, **96**, 4301–4306.

Meinnel,T., Sacerdot,C., Graffe,M., Blanquet,S. and Springer,M. (1999) Discrimination by *Escherichia coli* initiation factor IF3 against initiation on non-canonical codons relies on complementarity rules. *J. Mol. Biol.*, **290**, 825–837.

Moazed,D. and Noller,H.F. (1987) Interaction of antibiotics with functional sites in 16S ribosomal RNA. *Nature*, **327**, 389–394.

Moreau,M., De,C.E., Fortier,P.-L., Garcia,C., Albaret,C., Blanquet,S., Lallemand,J.-Y. and Dardel,F. (1997) Heteronuclear NMR studies of *E.coli* translation initiation factor IF3. Evidence that the inter-domain region is disordered in solution. *J. Mol. Biol.*, **266**, 15–22.

Mueller,F. and Brimacombe,R. (1997) A new model for the three-dimensional folding of *Escherichia coli* 16S ribosomal RNA. I. Fitting the RNA to a 3D electron microscopic map at 20 Å. *J. Mol. Biol.*, **271**, 524–544.

Nissen,P., Hansen,J., Ban,N., Moore,P.B. and Steitz,T.A. (2000) The structural basis of ribosome activity in peptide bond synthesis. *Science*, **289**, 920–930.

Noah,J.W., Dolan,M.A., Babin,P. and Wollenzien,P. (1999) Effects of tetracycline and spectinomycin on the tertiary structure of ribosomal RNA in the *Escherichia coli* 30S ribosomal subunit. *J. Biol. Chem.*, **274**, 16576–16581.

Nowotny,V. and Nierhaus,K.H. (1988) Assembly of the 30S subunit from *Escherichia coli* ribosomes occurs via two assembly domains which are initiated by S4 and S7. *Biochemistry*, **27**, 7051–7055.

O'Connor,M., Brunelli,C.A., Firpo,M.A., Gregory,S.T., Lieberman,K.R., Lodmell,J.S., Moine,H., VanRyk,D.I. and Dahlberg,A.E. (1995) Genetic probes of ribosomal RNA function. *Biochem. Cell Biol.*, **73**, 859–868.

O'Connor,M., Thomas,C.L., Zimmermann,R.A. and Dahlberg,A.E. (1997) Decoding fidelity at the ribosomal A and P sites: influence of mutations in three different regions of the decoding domain in 16S rRNA. *Nucleic Acids Res.*, **25**, 1185–1193.

Odon,O.W., Kramer,G., Henderson,A.B., Pinphanichakarn,P. and Hardesty,B. (1978) GTP hydrolysis during methionyl-tRNAf binding to 40S ribosomal subunits and the site of edeine inhibition. *J. Biol. Chem.*, **253**, 1807–1816.

Oehler,R., Polacek,N., Steiner,G. and Barta,A. (1997) Interaction of tetracycline with RNA: photoincorporation into ribosomal RNA of *Escherichia coli*. *Nucleic Acids Res.*, **25**, 1219–1224.

Orth,P., Saenger,W. and Hinrichs,W. (1999) Tetracycline-chelated Mg²⁺ ion initiates helix unwinding in Tet repressor induction. *Biochemistry*, **38**, 191–198.

Otwinowski,Z. and Minor,W. (1997) Processing of X-ray diffraction data collected in oscillation mode. *Acta Crystallogr. B*, **276**, 307–326.

Ringquist,S., Cunningham,P., Weitzmann,C., Formenoy,L., Pleij,C., Ofengand,J. and Gold,L. (1993) Translation initiation complex formation with 30S ribosomal particles mutated at conserved

positions in the 3′-minor domain of 16S RNA. *J. Mol. Biol.*, **234**, 14–27.

Roberts,M.C. (1996) Tetracycline resistance determinants: mechanisms of action, regulation of expression, genetic mobility and distribution. *FEMS Microbiol. Rev.*, **19**, 1–24.

Ross,J.I., Eady,E.A., Cove,J.H. and Cunliffe,W.J. (1998) 16S rRNA mutation associated with tetracycline resistance in a Gram-positive bacterium. *Antimicrob. Agents Chemother.*, **42**, 1702–1705.

Santer,M. *et al.* (1990) Base changes at position −792 of *Escherichia coli* 16S ribosomal-RNA affect assembly of 70s ribosomes. *Proc. Natl Acad. Sci. USA*, **87**, 3700–3704.

Schlünzen,F. *et al.* (2000) Structure of functionally activated small ribosomal subunit at 3.3 Å resolution. *Cell*, **102**, 615–623.

Sergiev,P.V., Lavrik,I.N., Wlasoff,V.A., Dokudovskaya,S.S., Dontsova, O.A., Bogdanov,A.A. and Brimacombe,R. (1997) The path of mRNA through the bacterial ribosome: A site-directed crosslinking study using new photoreactive derivatives of guanosine and uridine. *RNA*, **3**, 464–475.

Sette,M., Spurio,R., Van Tilborg,P., Gualerzi,C.O. and Boelens,R. (1999) Identification of the ribosome binding sites of translation initiation factor IF3 by multidimensional heteronuclear NMR spectroscopy. *RNA*, **5**, 82–92.

Shapkina,T.G., Dolan,M.A., Babin,P. and Wollenzien,P. (2000) Initiation factor 3-induced structural changes in the 30 S ribosomal subunit and in complexes containing tRNA(f)(Met) and mRNA. *J. Mol. Biol.*, **299**, 615–628.

Spahn,C.M.T. and Prescott,C.D. (1996) Throwing a spanner in the works: Antibiotics and the translation apparatus. *J. Mol. Med.*, **74**, 423–439.

Srivastava,S., Verschoor,A. and Frank,J. (1992) Eukaryotic initiation factor 3 does not prevent association through physical blockage of the ribosomal subunit–subunit interface. *J. Mol. Biol.*, **226**, 301–304.

Tapprich,W.E. and Hill,W.E. (1986) Involvement of bases 787–795 of *Escherichia coli* 16S ribosomal RNA in ribosomal subunit association. *Proc. Natl Acad. Sci. USA*, **83**, 556–560.

Tapprich,W.E., Goss,D.J. and Dahlberg,A.E. (1989) Mutation at position 791 in *Escherichia coli* 16S ribosomal RNA affects processes involved in the initiation of protein synthesis. *Proc. Natl Acad. Sci. USA*, **86**, 4927–4931.

Tedin,K., Moll,I., Grill,S., Resch,A., Graschopf,A., Gualerzi,C.O. and Blasi,U. (1999) Translation initiation factor 3 antagonizes authentic start codon selection on leaderless mRNAs. *Mol. Microbiol.*, **31**, 67–77.

Tocilj,A. *et al.* (1999) The small ribosomal subunit from *Thermus thermophilus* at 4.5 Å resolution: pattern fittings and the identification of a functional site. *Proc. Natl Acad. Sci. USA*, **96**, 14252–14257.

VanLoock,M.S., Agrawal,R.K., Gabashvili,I.S., Qi,L., Frank,J. and Harvey,S.C. (2000) Movement of the decoding region of the 16S ribosomal RNA accompanies tRNA translocation. *J. Mol. Biol.*, **304**, 507–515.

Walsh,C. (2000) Molecular mechanisms that confer antibacterial drug resistance. *Nature*, **406**, 775–781.

Weiel,J. and Hershey,J.W. (1981) Fluorescence polarization studies of the interaction of *Escherichia coli* protein synthesis initiation factor 3 with 30S ribosomal subunits. *Biochemistry*, **20**, 5859–5865.

Wimberly,B., Brodersen,D., Clemons,W., Morgan-Warren,R., Carter,A., Vonrhein,C., Hartsch,T. and Ramakrishnan,V. (2000) Structure of the 30S ribosomal subunit. *Nature*, **407**, 327–339.

Woodcock,J., Moazed,D., Cannon,M., Davies,J. and Noller,H.F. (1991) Interaction of antibiotics with A-site-specific and P-site-specific bases in 16S ribosomal RNA. *EMBO J.*, **10**, 3099–3104.